Effects of Ferrocene on Production of High Performance Carbon Electrodes from Poly(furfuryl alcohol)

Jun-ichi Ozaki,*,† Masahiko Mitsui,† Yoshiyuki Nishiyama,†
John D. Cashion,‡ and L. Joan Brown‡

Institute for Chemical Reaction Science, Tohoku University, Katahira, Aoba-ku, Sendai 980-77, Japan, and Department of Physics, Monash University, Clayton, Victoria 3168, Australia

Received February 10, 1998. Revised Manuscript Received August 10, 1998

The properties and structure of mixtures of ferrocene and poly(furfuryl alcohol) (PFA) were studied on carbonizing it at different temperatures up to 800 °C. Samples carbonized above 700 °C showed high heterogeneous electron transfer rates comparable to that of a platinum electrode, when these were used as working electrodes in cyclicvoltammetric studies of ferricyanide. Furlike structure was observed under SEM for these carbonized mixtures and the high electrochemical activity attributed to this structure. Mössbauer spectroscopy revealed that the introduced ferrocene had decomposed by 300 °C and was initially converted to magnetite, then to wustite, and finally to a mixture of α- and γ-iron and cementite. The electrical conductivity of the carbonized, iron-containing mixture was higher than that of the carbonized pure PFA by 1 order of magnitude for all the heat treatment temperatures investigated. The conductivity changed from an activated mechanism to metallic type at 700 °C heat treatment temperature. The major role of the introduced iron was considered to be to dissolve carbon atoms during heat treatment and then to deposit the filamentary carbon on cooling.

I. Introduction

On heat treatment at lower than 1000 °C, some organic substances can be transformed into solid carbonaceous materials. This results from the elimination of heteroatoms such as H, O, S, N, and halogens, and from aromatization to make condensed aromatic structures. Usually these processes are collectively called carbonization, distinguishing it from graphitization, which gradually occurs at higher temperatures than 1000 °C.[1] The electronic properties of carbonaceous materials dramatically change during the carbonization process; for example, the electrical conductivity of the carbonaceous materials increases by 10 orders of magnitude during this process.[2] This large change suggests that one may obtain electronically functional materials by controlling the preparations.

We have been interested in the variations of the electronic properties of carbons during carbonization, and have been engaged in developing low-temperature carbons with electronic functions by controlling their preparation.[2−9] Besides altering the conditions such as atmosphere and temperature for carbonization, the addition of metal elements to the carbonizing systems should be effective, because metal elements are known to affect reactions involving carbon, for example, catalytic graphitization,[10−18] catalytic gasification,[19] and carbon deposition onto metal surfaces.[20,21]

Controlling the properties of carbons by introducing an iron complex to carbonization systems has been the subject in which we have been interested. The effects obtained from the introduction of iron were as follows: (1) increased electrical conductivity of carbonized poly(vinylidene chloride) at 400 °C by 10 orders of magnitude,[6] (2) enhanced photovoltaic response of carbon/n-Si junctions made by plasma decomposition of propylene,[7] and (3) yielded a highly active carbon working electrode.[8,9] The results concerning the third effect are briefly reviewed below.

* Present address of corresponding author: Faculty of Engineering, Gunma University, Kiryu, Gunma 376, Japan.
† Tohoku University.
‡ Monash University.

(1) For example: Spain, I. L. *Chemistry and Physics of Carbon*; Walker, P. L., Jr., Thrower, P. A., Eds.; Dekker: New York, 1981; Vol. 16, p 119. Delhaes, P., Carmona, F. *Chemistry and Physics of Carbon*; Walker, P. L., Jr., Thrower, P. A., Eds.; Dekker: New York, 1981; Vol. 17, p 89. Emmerich, F. G.; Soysa, J. C.; Torriani, I. L.; Luengo, C. A. *Carbon* **1987**, *25*, 417.
(2) Ozaki, J.; Nishiyama, Y. *Carbon* **1987**, *25*, 697.
(3) Ozaki, J.; Nishiyama, Y. *J. Appl. Phys.* **1989**, *65*, 2744.
(4) Ozaki, J.; Sunami, I.; Nishiyama, *Y. J. Phys. Chem*. **1990**, *94*, 3839.
(5) Ozaki, J.; Nishiyama, Y. *J. Appl. Phys*. **1991**, *69*, 324.
(6) Ozaki, J.; Watanabe, T.; Nishiyama, Y. *J. Phys. Chem*. **1993**, *97*, 1400.
(7) Ozaki, J.; Nishiyama, Y. *J. Appl. Phys*. **1995**, *77*, 4459.
(8) Ozaki, J.; Mitsui, M.; Nishiyama, Y. *Tanso* **1994**, *165*, 268.
(9) Ozaki, J.; Mitsui, M.; Nishiyama, Y. *Carbon* **1998**, *36*, 131.
(10) Marsh, H.; Waburton, A. P. *J. Appl. Chem*. **1970**, *20*, 133.
(11) Oberlin, A.; Rouchy, J. P. *Carbon* **1971**, *9*, 39.
(12) Courtney, R. L.; Duliere, S. F. *Carbon* **1972**, *10*, 65.
(13) Baraniecki, C.; Pinchbeck, P. H.; Pickering, F. B. *Carbon* **1969**, *7*, 213.
(14) Otani, S.; Oya, A.; Nishinou, M. *Tanso* **1974**, *1974*, 2.
(15) Oya, A.; Otani, S. *Carbon* **1978**, *16*, 15.
(16) Oya, A.; Mochizuki, M.; Otani, S. *Carbon* **1979**, *17*, 71.
(17) Oya, A.; Marsh, H. *J. Mater. Sci.* **1982**, *17*, 309.
(18) Oya, A.; Jikihyara, S.; Otani, S. *Fuel* **1983**, *62*, 50.
(19) Nishiyama, Y. *Fuel. Proc. Technol*. **1991**, *29*, 31.
(20) Nishiyama, Y. *Sekiyu Gakkaishi* **1974**, *17*, 454.
(21) Nishiyama, Y.; Tamai, Y. *CHEMTECH* **1980**, *1980*, 680.

10.1021/cm980081m CCC: $15.00
Published on Web 09/26/1998

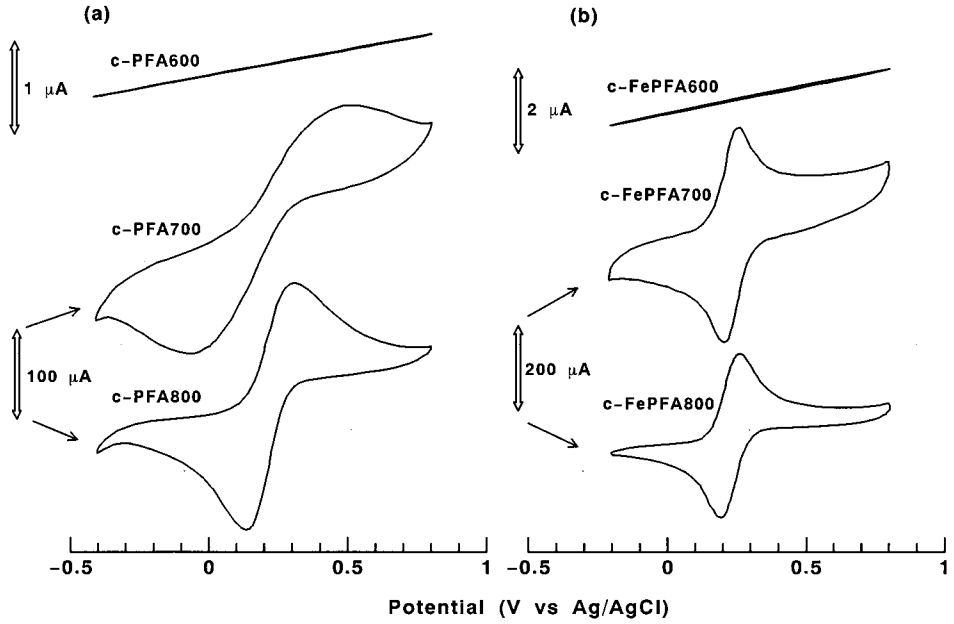

Figure 1. Cyclic voltammograms of carbon working electrodes in an aqueous solution of 6×10^{-3} mol/dm^3 $K_3[Fe(CN)_6]$ with 1 mol/dm^3 KCl supporting electrolyte. The potential sweep rate was 10 mV/s. (a) c-PFA series, (b) c-FePFA series samples.

In the previous studies, iron-containing carbons were prepared from the mixtures of poly(furfuryl alcohol) (PFA) and ferrocene by carbonizing them at 700 °C, and their electrochemical behavior as working electrodes was assessed with a redox reaction of ferricyanide by cyclic voltammetry. Ferrocene was selected as an iron source as this compound contains only C and H other than Fe. It has been revealed that the composites thus made showed fast rates of electron-transfer comparable to a platinum electrode.[8] PFA was found not to be a unique polymer for preparing this type of electrochemically active carbon in the presence of ferrocene, as resol-type phenolic resin also showed such activity. The common features of the iron−carbon composites between the PFA origin and phenolic resin origin were their turbostratic X-ray diffractions and furlike mophologies.[9] As these features were very similar to the T_s-phase, which was found by Oya et al. in the studies on catalytic graphitization,[17] we inferred that this special type of carbon, T_s-phase, would be responsible for the high electrochemical activity found for our iron−carbon materials.

In this study, the effect of the introduced ferrocene on the carbonization of PFA was investigated from the viewpoints of the electronic properties and the variation in iron chemical states with varying carbonization temperature.

II. Experimental Section

Sample Preparation. A mixture of PFA and ferrocene was prepared by the following procedure: ferrocene was dissolved in furfuryl alcohol and it was then polymerized by adding hydrochloric acid as an initiator at 80 °C for 48 h. The amount of ferrocene was such as to give 3 wt % iron in the starting polymer. This mixture, which we shall refer to as FePFA, was heat treated in a helium stream at different temperatures between 200 and 800 °C for 1 h with a heating rate of 150 °C/h. PFA, without ferrocene, was also prepared as a control by performing the same heat treatment as for the FePFA case. Hereafter, the heat-treated samples are labeled by prefixes "c", as in c-PFA or c-FePFA, followed by the heat treatment temperature. The carbonized samples were pulverized and sieved into particles of diameter less than 100 μm.

Characterization. ^{57}Fe Mössbauer spectra were obtained, mainly at room temperature, using a conventional symmetrical triangular velocity waveform to drive a ^{57}Co in Rh source. Scanning electron microscopy and X-ray diffraction were also applied to several samples.

Cyclic Voltammetry. The electrochemical characteristics of the carbons were evaluated by cyclic voltammetry of a redox reaction of the ferricyanide anion in an aqueous solution of $K_3[Fe(CN)_6]$ (6×10^{-3} mol/dm^3) with 1 mol/dm^3 of KNO_3 as a supporting electrolyte. The working electrodes were fabricated on a stainless steel backing, which acted as a current collector, by impregnating the carbon powder with a Teflon dispersion binder. The electrode assembly was set on a glass flange of the electrochemical cell via an O-ring. The apparent area of the working electrode was 0.28 cm^2. An Ag/AgCl electrode was used as a reference electrode. The electrolyte was deaerated by bubbling with nitrogen gas before the measurements. The cyclic voltammograms were recorded between −0.4 and +1.0 V vs Ag/AgCl and with varying potential sweep rates between 5 and 100 mV/s. To obtain reference cyclic voltammograms, CV runs were performed with the same electrolyte solution by employing a platinum plate as a working electrode.

Electrical Conductivity. The electrical conductivity of the powder samples was measured by using a specially designed device consisting of two 5 mm diameter copper plungers inside a cylinder of canvas Bakelite. One of the plungers was fixed to the cylinder and the other was spring loaded to give a reproducible force. The powder sample, approximately 0.5 mm thick, was charged between the plungers. The device was mounted on a long rod which could be inserted into a liquid helium container via a sliding O-ring fitting. Adjusting the height of the rod allowed continuous variation of the measurement temperature, which was monitored by an AuFe thermocouple. The electrical conductivity was calculated from the applied field and the current density between the two plungers.

III. Results

Electrochemical Properties. Figure 1 shows the cyclic voltammograms of the carbons at a sweep rate of 10 mV/s. An almost straight line was obtained for c-PFA600 without any redox peaks. When this sample is heat treated at 700 °C, the cyclic voltammogram

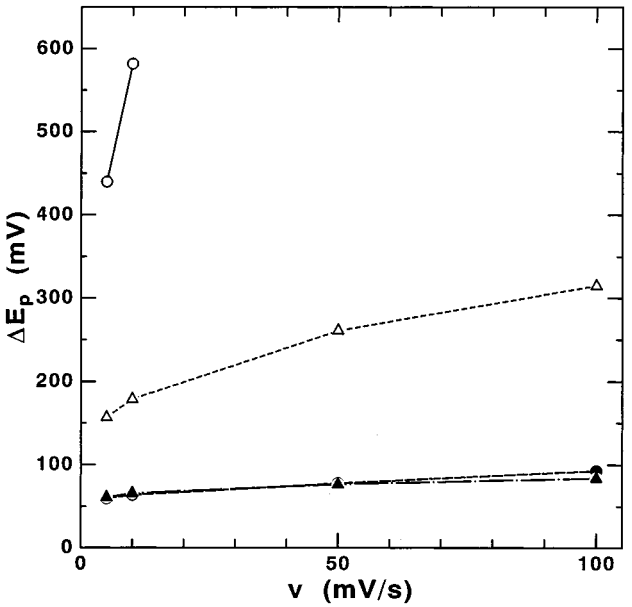

Figure 2. Dependence of ΔE_P on the potential sweep rate. Open circle, c-PFA700; open triangle, c-PFA800; filled circle, c-FePFA700; filled triangle, c-FePFA800.

changes into the one with obvious redox peaks. On heat treatment at 800 °C, both reduction and oxidation waves are clearly developed. For the c-FePFA samples, there were also no redox peaks after treatment at 600 °C, as in the case of c-PFA600. A drastic change in the voltammogram is seen after heat treatment at 700 °C, with the development of sharp redox waves. Almost no changes on the Faradaic currents occurred between c-FePFA700 and -800, except for the magnitudes of the non-Faradaic current. This difference would be caused probably by the packing state of the carbons on the stainless backing metals for working electrodes. We shall not discuss this difference further.

In general, the peak separation between the oxidation peak and the reduction peak, ΔE_P, in cyclic voltammograms is a measure of the reversibility of the electrochemical reaction.[22] Figure 2 shows the dependence of ΔE_P on the sweep rate, v, for the four samples for which the redox peaks could be defined. With increasing heat treatment temperature from 700 to 800 °C, the ΔE_P of the c-PFA samples decreased and the change with v became smaller, which indicates that the electron transfer across the interface between the electrode and the redox couple is too slow to catch up with the potential sweep. The ΔE_P values of the c-FePFA samples were smaller than those of the c-PFA samples and showed almost no dependence on v. Furthermore, it should be noted that the ΔE_P values of the FePFA samples were about 60 mV, which is close to the value for the reversible case, 59 mV,[22] showing that the heterogeneous electron transfer at the surfaces of these carbons occurred at high rates. The heterogeneous electron-transfer rates, calculated by the method proposed by Nicholson,[23] are tabulated in Table 1 together with the value calculated from the voltammogram with a Pt plate electrode employed in order to obtain a reference for comparison. Here, we would like to emphasize again that the electron-transfer rates of c-FePFA700 and -800 are comparable to those for platinum electrodes, within the error of the analysis.

Table 1. Heterogeneous Electron Transfer Rates

sample	k_S (10^{-3} cm/s)	sample	k_S (10^{-3} cm/s)
c-PFA600	na[a]	c-FePFA600	na
c-PFA700	na	c-FePFA700	29
c-PFA800	0.6	c-FePFA800	28
		Pt	13

[a] na: Nicholson's method not applicable.

Table 2. Room Temperature Electrical Conductivity

heat treatment temperature (°C)	c-PFA (S/cm)	c-FePFA (S/cm)
300		4.7×10^{-12}
400	1.0×10^{-11}	1.3×10^{-10}
500	3.9×10^{-9}	2.0×10^{-8}
600	1.2×10^{-6}	1.9×10^{-5}
650		2.7×10^{-3}
700	2.2×10^{-2}	1.9
800	0.44	2.6

Electrical Conductivity. A comparison of the room-temperature conductivity between c-PFA samples and c-FePFA samples is made in Table 2. In the case of c-PFA series, although the conductivity of c-PFA300 was too low for our measuring system, the conductivity ranges over 10 orders of magnitude. A maximum change of the conductivity per 100 °C increment of the heat-treatment temperature is observed between 600 and 700 °C. The conductivity changes for the c-FePFA series also ranges over the same magnitude as for c-PFA, although the conductivity of the samples of this series is generally greater than the conductivity of the corresponding c-PFA samples by an order of magnitude. The increment of the conductivity between c-FePFA600 and -700 is 5 orders of magnitude, which is larger than the case of c-PFA series.

The temperature dependence of the conductivity of the carbonized samples is presented as an Arrhenius-type plot in Figure 3. The electrical conductivity of the c-PFA samples decreased with reduced measurement temperature, implying that the conduction mechanisms of these materials included activation processes. With increasing heat treatment temperature, the straight Arrhenius plots observed for the samples with lower heat treatment temperatures became curved and the maximum slope of the plot is decreased. Curved Arrhenius plots indicate a variety of conduction mechanisms, among which the dominant mechanism changes, depending on the measurement temperature.

The Arrhenius plot of c-FePFA samples carbonized at a temperature up to 600 °C also show that the conduction is governed by several types of activation processes. The c-FePFA650 sample shows an interesting feature, namely a temperature independent, metallic type conduction at low temperatures, with an activated conduction mechanism coming in additionally at higher temperatures. The samples of c-FePFA700 and -800 show almost constant conductivity independent of the measurement temperature, which indicates the occurrence of metallic conduction.

Scanning Electron Microscopy. Figure 4 shows the scanning electron images of the samples prepared at temperatures between 600 and 700 °C. The appear-

(22) Bard, A. J.; Faulkner, L. R. *Electrochemical Methods*; John Wiley: New York, 1980; p 227.
(23) Nicholson, R. S. *Anal. Chem.* **1965**, *37*, 1351.

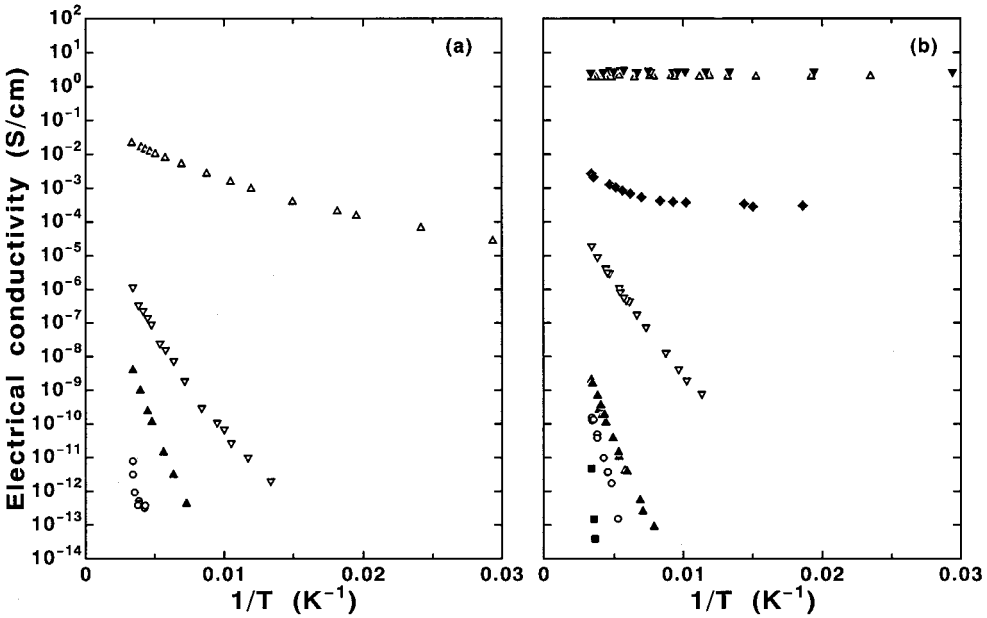

Figure 3. Dependence of electrical conductivity on the measurement temperature of (a) c-PFA and (b) c-FePFA. The following symbols stand for the heat treatment temperatures and are common for both plots: closed square, 300 °C; open circle, 400 °C; closed triangle, 500 °C; open inverse triangle, 600 °C; closed rhombus, 650 °C; open triangle, 700 °C; closed inverse triangle, 800 °C.

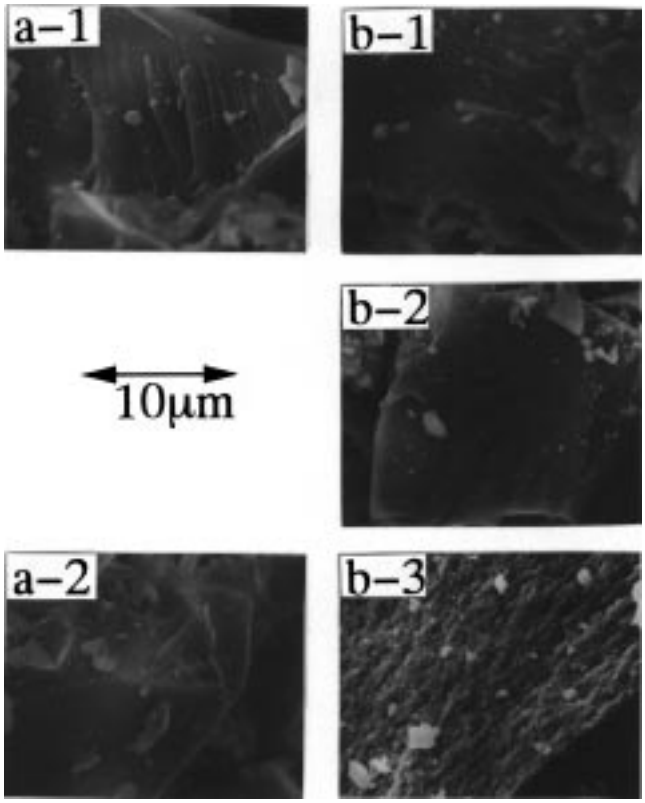

Figure 4. Scanning electron micrographs of carbonized poly(furfuryl alcohol): (a-1) c-PFA500, (a-2) c-PFA700, (b-1) c-FePFA500, (b-2) c-FePFA600, (b-3) c-FePFA700.

ance of c-PFA samples under the electron microscope was not changed by further heat treatment above 600 °C, i.e., these have hard and smooth surfaces characteristic of glasslike carbons. The surfaces of c-FePFA samples prepared at temperatures lower than 700 °C showed similar surfaces to those of c-PFA samples. However, after the heat treatment at 700 °C, the hard and smooth surfaces suddenly changed to a furlike structure that was also seen for c-FePFA800. The furlike structure of c-FePFA700 was reported in previous papers.[8,9]

Mössbauer Spectroscopy. The room temperature ^{57}Fe Mössbauer spectra of the c-FePFA samples are presented in Figure 5 and the results of the analyses of the spectra are tabulated in Table 3. The transformations of the iron species break up into four distinct groups.

The dominant phase in the spectrum of c-FePFA200 is due to ferrocene, with two other doublets being present. The more intense of these is due to the ferrocenium ion in a form with parameters similar to those of methyl diferrocenium, while the second, labeled doublet 3, has not been identified. After 250 °C heat treatment, the proportion of ferrocene has been halved while the unidentified doublet has increased considerably.

A dramatic change occurred after heating the sample to 300 °C, with the spectrum now being composed principally of the two overlapping sextets of magnetite, Fe_3O_4. This situation persisted until the 600 °C heating, which reduced all the iron into wustite, $Fe_{1-x}O$. Further transformation occurred after heating to 650 °C when about one-third of the wustite had been transformed, principally into α-iron and cementite, Fe_3C. Comparison with the spectra of Greenwood and Howe[24] and McCammon and Price[25] shows that the wustite composition in c-FePFA600 is approximately $Fe_{0.98}O$ while in c-FePFA650 it is stoichiometric FeO with no Fe^{3+} peak. Further heating caused the proportion of cementite to increase steadily with treatment temperature while the proportion of α-iron reached a maximum and then decreased due to the formation of γ-iron.

(24) Greenwood, N. N.; Howe, A. T. *J. Chem. Soc., Dalton* **1972**, 110.
(25) McCammon, C. A.; Price, D. C. *Phys. Chem. Min.* **1985**, *11*, 250.

Table 3. Fitted Parameters for the Mössbauer Spectra in Figure 5

HTT[a]	ferrocene			ferrocenium			doublet 3			Fe_3O_4			$Fe_{1-x}O$		Fe_3C			α-Fe			γ-Fe	
(°C)	δ	Δ	A%	δ	Δ	A%	δ	Δ	A%	δ	H(T)	A%	δ	A%	δ	H(T)	A%	δ	H(T)	A%	δ	A%
200	0.43	2.29	52	0.34	0.73	37	1.01	2.17	11													
250	0.44	2.29	25	0.37	0.72	33	1.03	2.11	42													
300				0.29	0.75	8				0.27	48.6	31	1.08	6								
										0.66	45.8	56										
400				0.34	0.91	2				0.28	48.7	34	1.09	2								
										0.66	45.9	62										
500				0.32	1.47	3				0.27	48.8	33	1.07	3								
										0.66	45.9	61										
600													1.06	75								
													0.59	25								
650													1.04	67	0.22	20.9	11	0.00	33.2	20	−0.13	2
680													1.06	12	0.18	20.6	51	0.00	33.2	29	−0.11	9
700															0.19	20.7	66	0.00	33.2	22	−0.10	12
800															0.18	20.9	70	0.00	33.4	16	−0.11	14

[a] Carbonization temperature.

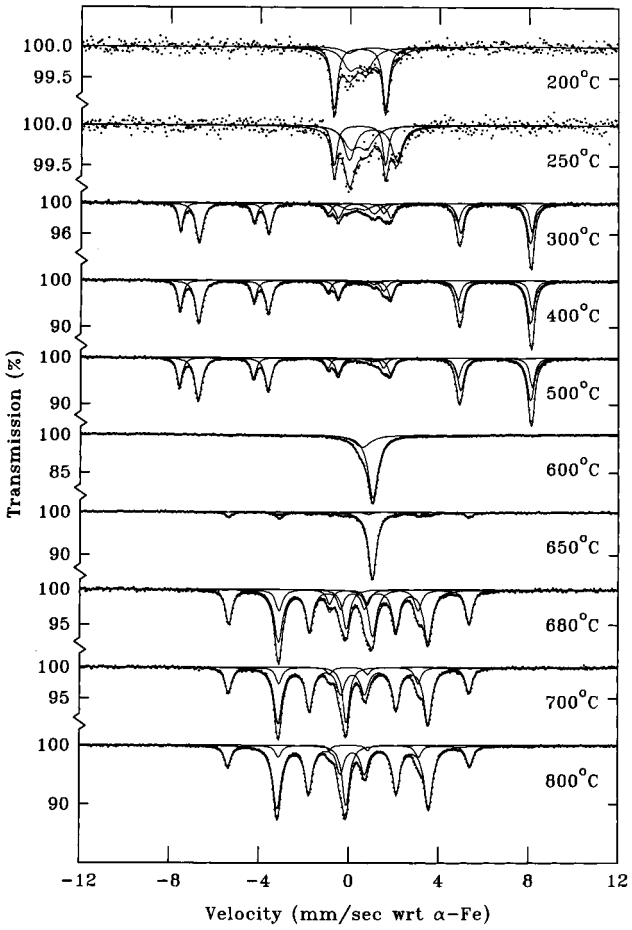

Figure 5. Room-temperature Mössbauer spectra of c-FePFA samples heat treated to the temperatures shown.

IV. Discussion

Evolution of Iron Species and Formation of Furlike Structure. The evolution of iron species detected by Mössbauer spectroscopy can be summarized as follows. The initial compound, ferrocene, was converted to ferrocenium ion and an unknown species denoted as doublet 3 in Table 3. During the treatment between 300 and 500 °C, the major species was magnetite, which was converted into wustite at 600 °C. Above 700 °C, where the electrochemical activity was obtained and the furlike structure appeared, we had the three species, α-Fe, γ-Fe, and cementite.

A feature of the series of spectra shown in Figure 5 that deserves note is the very large variation in the recoilless fraction at room temperature of the samples. All the spectra in Figure 5 were taken with approximately constant mass and the intensity of the absorption rises by a factor of 18 between the 200 and 250 °C spectra of ferrocene and ferrocinium and the 400 and 500 °C spectra of magnetite. The area then decreases by over a factor of 2 during the reduction to wustite and α-iron at 650 °C. The production of cementite produces a very rapid increase of a factor of 2.5 in the spectral area over the heating to 680 °C and another significant increase of 10% between 700 and 800 °C. Some of the increase in area will be due to the increase in iron content in the constant mass samples due to the elimination of heteroatoms, but the decrease in intensity accompanying the reduction of the magnetite is quite striking. We believe that these very large changes are indicative, principally, of bonding changes in the transition from ferrocene/ferrocinium to magnetite and of particle size changes in the oxide/metal/carbide samples. The results indicate that the recoilless fractions may be very different for the species present in any particular spectrum, and hence the common assumption that spectral areas represent, to a good approximation, the proportion of iron in each phase may be subject to quite large errors in this case.

It is interesting to note that the Mössbauer spectra of the c-FePFA samples treated above 250 °C all show well-formed line shapes, which indicate good crystallinity throughout, despite the changes in recoilless fraction and inferred particle size changes. Magnetite frequently produces poorly resolved spectra in cases where reactions are proceeding, such as in coal carbonization and iron ore direct reduction processes. The good quality of the spectra is probably also evidence of considerable agglomeration of the iron species during the carbonization process.

The importance of the presence of metal particles has been pointed out in the formation of carbons with special structures, such as filamentous carbons deposited on metal surfaces,[26] or nanoparticles and nanotubes which were found as the byproducts of fullerenes.[27] Baker[26] claimed that the initial step of the formation of fila-

(26) Baker, R. T. K.; Waite, R. J. *J. Catal.* **1975**, *37*, 101.
(27) Saito, Y. *Carbon* **1995**, *33*, 979.

mentous carbons on metal particles is the decomposition of hydrocarbon on the particle into atomic carbon. Then the adsorbed carbon atoms dissolve into the particles to be segregated from the other surface of the particle. Saito et al.[27] explained the formation of metal-filled carbon nanoparticles or nanotubes by the following mechanism: particles of metal−carbon alloy in a liquid state are first formed on the surface of a cathode for arc discharge, and then the graphitic carbon segregates on the surface of the particles with decreasing temperature. In both mechanisms, segregation of graphitic carbon from metal−carbon solutions plays an important role to form such particular forms of carbons.

In the present study, we found Fe_3C, γ-Fe, and α-Fe in the samples with higher electrochemical activity by using Mössbauer spectroscopy. Although these species were observed in samples taken out of the furnace, they give us implications on the interactions between metal and carbon at the working state. In metallurgy, the solid solution of iron and carbon gives α-Fe and Fe_3C. In the present case, the Mössbauer spectra detected the presence of γ-iron, which is only thermodynamically stable at temperatures above 911 °C,[28] but dissolution of carbon reduces this limit and it can then be quenched to room temperature. We do not yet fully understand the interrelationship among the three species, α-Fe, γ-Fe, and Fe_3C, but it is likely that the cooling causes the exsolution of some of the carbon from the γ-iron, resulting in the formation of the furlike structure observed in the SEM. If this is true, the formation of the furlike carbon should depend on the cooling rate after carbonization, and further work is being carried out on this subject.

Electrical Conduction of Carbons. Curved Arrhenius plots were observed for the c-PFA samples and for the c-FePFA samples that were prepared lower than 700 °C. Carmona et al. found a curved behavior for anthracene chars[29] and explained it by a transition in the conduction mechanism, from a thermally assisted hopping mechanism to a variable range hopping mechanism with decreasing measurement temperature. The present authors recently found that the electrical conductivity depends exponentially on the separation distance between the aromatic moieties in carbonaceous materials.[30,31] So, we believe a hopping conduction mechanism is more plausible than band conduction in these low temperature prepared carbons, with the slope of the Arrhenius plots representing the weighted average activation energy of the mechanisms available at that temperature.

The electrical conduction of carbons changes with heat treatment, from semiconductor type to metal type conduction, reflecting the fact that the electronic structure of carbon approaches that of graphite, a semimetal, with heat treatment.[1] The introduction of iron was found to promote the conversion from the semiconductor-type conduction to the metal-type one, as can be seen in Figure 3.

Origin of the High Electrochemical Activity. Here we show some parallelism between the electrical conductivity and ΔE_P of carbonized samples: i.e., it looks as if the increase in the electrical conductivity leads to the decrease in ΔE_P. We should remember that the potentiostat regulates the potential of the current collector rather than that of the surface of the bound carbon samples on the collector. So, the actual potential of the surface of the electrode is different from the potential set by the potentiostat because of an IR drop occurring across the carbon layer. This potential difference should be smaller when a carbon with high conductivity is used as the working electrode material, while the difference would be significant for carbons with low conductivity. In the latter case, a broadened cyclic voltammogram will be obtained.

If the increase in the electrical conductivity is a factor that is responsible for the decrease in ΔE_P, i.e., increase in k_S, then a working electrode made with graphite should give the highest heterogeneous electron-transfer rate. In our previous study, the graphite electrode did not show as high activity as a c-FePFA sample.[8] Furthermore, we should recognize the difference in the chemical reactivity of two principal crystallographic directions in the graphite crystal, i.e., parallel and perpendicular to the basal plane. When one cleaves the crystal perpendicular to the *c*-axis, the bond broken is van der Waals' bond. However, cutting parallel to the *c*-axis, one must break the covalent bond, which forms defects, such as dangling bonds, leading to unsaturated coordination of the carbon atoms. These differences are responsible for the anisotropy in the chemical reactivity of the graphite crystal. Thus, the electrochemical activity of the end surfaces was found to be higher than that of the basal plane.[32]

We tentatively explain the high heterogeneous electron-transfer rate obtained for c-FePFA700 and -800 carbons as follows. These carbons have a structure which enables higher exposure of the end surfaces. To clarify the origin of the high electrochemical activity of the series of materials, we need to perform detailed TEM observations to investigate the particular structure or to measure oxygen adsorption TPD (temperature programmed desorption) spectra.

V. Conclusion

In this study, we have investigated the carbonization of poly(furfuryl alcohol) mixed with ferrocene from the viewpoints of electrochemical activity, morphological changes under SEM, electrical conductivity, and Mössbauer spectroscopy of the incorporated iron. The electrochemical activity (assessed by heterogeneous electron-transfer rate) and the characteristic furlike morphology were found to appear when the mixed raw material was carbonized above 700 °C. Around the same temperature, the conduction type changed from an activated one to a metallic one. During these transitions from the lower temperature phase to the higher temperature one, wustite formed by 600 °C was transformed to the three phases α-Fe, γ-Fe, and cementite, the latter two phases involving iron−carbon interactions. We propose that

(28) Okamaoto, H. *Phase Diagrams of Binary Iron Alloys*; ASM International: Materials Park, OH, 1993; p 64.
(29) Carmona, F.; Delhaes, P.; Keryer, G.; Manceau, J. P. *Solid State Commun.*, **1974**, *14*, 1183.
(30) Ozaki, J.; Nishizawa, S.; Nishiyama, Y. *Carbon* **1997**, *35*, 45.
(31) Ozaki, J.; Nishiyama, Y.; Cashion, J. D.; Brown, L. J. *Fuel*, in press.
(32) Wightman, R. M.; Deakin, M. R.; Kovach, P. M.; Kuhr, W. G.; Stutts, K. J. *J. Electrochem. Soc.* **1984**, *131*, 1579.

the segregation of some of the carbon from the carbon−iron solution is responsible for the production of the furlike material. Finally, the decrease in ΔE_P should be mainly caused by the surface structure of the carbon, although the electrical conductivity of the bulk electrode carbon will also contribute to the decrease.

Acknowledgment. The authors are grateful for the financial support of Monbusho, the Monash University Research Fund, and the Australian Research Council.

CM980081M